agronomy

MDPI

Article

Prediction and Impact Analysis of Soil Nitrogen and Salinity Under Reclaimed Water Irrigation: A Case Study

Zeyu Liu [1], Kai Fang [2], Xiaoqin Sun [3], Yandong Wang [2], Zhuo Tian [3], Jing Liu [4], Liying Bai [5] and Qilin He [3,*]

[1] Reading Academy, Nanjing University of Information Science & Technology, Nanjing 210044, China
[2] Suqian Water Conservation Management Service Center, Suqian 223800, China
[3] College of Soil and Water Conservation, Hohai University, Nanjing 210098, China
[4] Suqian Research Institute, Hohai University, Suqian 223800, China
[5] Zhenjiang Branch of Jiangsu Provincial Hydrology and Water Resources Survey Bureau, Zhenjiang 212080, China
* Correspondence: heqilin@hhu.edu.cn

Abstract: Reclaimed water irrigation is increasingly being applied to address global water scarcity, yet its long-term effects on soil nitrogen cycling and salinity dynamics, particularly in agricultural and agroforestry systems, remain complex and insufficiently understood. Understanding these impacts is crucial for developing sustainable practices that optimize resource use while ensuring the long-term health and viability of agricultural and agroforestry systems. This study employs genetic-algorithm-optimized random forest models (GA-RF1 and GA-RF2) to examine the dynamics of nitrogen indicators (NO_3^--N, NH_4^+-N, and TN) and salinity indicators (EC and Cl^-) under reclaimed water irrigation. The models achieved high predictive accuracy, with NSE values of 0.918, 0.946, 0.936, 0.967, and 0.887 for NO_3^--N, NH_4^+-N, TN, EC, and Cl^-, respectively, demonstrating their robustness. Key drivers of nitrogen indicators were identified as irrigation duration (years), fecal coliform levels, and soil depth, while salinity indicators were primarily influenced by land use type and the chemical composition of reclaimed water, including chemical oxygen demand, total phosphorus, and total nitrogen. Spatial analysis revealed significant nitrogen and salinity accumulation in surface soils with extended irrigation, particularly in farmland, where NO_3^--N and NH_4^+-N peaked at 25 mg/kg and 15 mg/kg, respectively. EC exceeded 700 μS/cm during early irrigation stages but remained within crop tolerance levels. Conversely, grassland and woodland exhibited minimal nitrogen and salinity accumulation. These findings underscore the need for targeted management strategies to mitigate nitrogen and salinity buildup, particularly in farmland, to ensure long-term soil health and productivity under reclaimed water irrigation systems.

Keywords: reclaimed water irrigation; nitrogen indicators (NO_3^--N, NH_4^+-N, TN); salinity indicators (EC, Cl^-); genetic-algorithm-optimized random forest (GA-RF)

check for updates

Academic Editor: Belen Gallego-Elvira

Received: 2 December 2024
Revised: 24 January 2025
Accepted: 28 January 2025
Published: 11 February 2025

Citation: Liu, Z.; Fang, K.; Sun, X.; Wang, Y.; Tian, Z.; Liu, J.; Bai, L.; He, Q. Prediction and Impact Analysis of Soil Nitrogen and Salinity Under Reclaimed Water Irrigation: A Case Study. *Agronomy* **2025**, *15*, 443. https://doi.org/10.3390/agronomy15020443

Copyright: © 2025 by the authors. Licensee MDPI, Basel, Switzerland. This article is an open access article distributed under the terms and conditions of the Creative Commons Attribution (CC BY) license (https://creativecommons.org/licenses/by/4.0/).

1. Introduction

Irrigated agriculture is essential for addressing the growing global water scarcity, particularly in developing countries where access to fresh water is increasingly limited [1,2]. Clean water scarcity is a growing issue, affecting 47% of the global population, or 3.6 billion people, who live in regions with water scarcity for at least one month each year. By 2050, with the world population expected to rise from 22 to 34%, the strain on water resources will intensify, particularly in developing countries in Africa and Asia, where clean water scarcity is already a significant problem [3,4]. Insufficient irrigation infrastructure and

water availability in agriculture lead to decreased crop yields, reduced productivity, and soil degradation [5]. Declining soil moisture limits plant growth, increases erosion, nutrient loss, and structural degradation, and raises crop failure rates, especially in drought-prone areas [6]. This threatens food security and farmer livelihoods, highlighting the urgent need for effective water management and sustainable irrigation practices.

In this context, reclaimed wastewater is emerging as a critical solution to alleviate pressure on freshwater resources [7]. Reclaimed water, compared to untreated wastewater, presents significantly lower pollution risks while providing essential nutrients such as nitrogen, phosphorus, and potassium, which support plant growth. Its use in irrigation not only reduces pollutant discharge into water systems, but also lowers fertilizer dependence and improves soil quality, delivering substantial environmental benefits in agriculture and green space management [8,9]. However, the use of reclaimed water for irrigation presents potential challenges, particularly regarding the accumulation of nitrogen and salts in the soil. These processes, if not properly managed, can affect soil health and water quality, potentially impacting the long-term viability of agricultural and agroforestry systems [10,11]. To ensure sustainable and efficient resource use, it is crucial to understand the mechanisms of nitrogen and salt dynamics under reclaimed water irrigation. This knowledge is essential for optimizing irrigation practices, safeguarding long-term ecosystem health, and promoting the sustainable development of agricultural and agroforestry systems.

Understanding these mechanisms requires examining how various factors interact to influence nitrogen and salt accumulation. Research has demonstrated that water quality, irrigation practices, soil properties, and land use patterns play critical roles in shaping these dynamics [12–16]. Reclaimed water irrigation significantly impacts soil properties, enhancing nutrient levels such as phosphorus and nitrogen while increasing salt concentrations. Studies show that deeper soil layers tend to accumulate more salts under full irrigation [16], and prolonged use raises soil electrical conductivity and sodium content [12]. Land use and vegetation types influence these outcomes, with perennial crops like grapes and almonds exhibiting lower salinity levels compared to horticultural crops [15], while grasslands show gradual increases in salinity and sodium adsorption ratios over time [17]. Tailored management strategies, including optimizing irrigation schedules, improving water quality, and adapting land use practices, are essential to balance nutrient and salinity levels, supporting the long-term sustainability of agricultural and agroforestry systems.

Although field observations and laboratory analyses have shed light on the effects of water quality, irrigation practices, soil properties, and land use patterns on soil nitrogen and salinity under reclaimed water irrigation [12–14,16], most studies have focused on individual factors, with limited exploration of their interactions. Moreover, the relative importance of these factors in driving soil nitrogen and salinity dynamics remains unclear. Advances in data science have introduced machine learning methods, such as random forest (RF) models, as powerful tools for studying soil quality and nutrient dynamics. RF models effectively assess variable importance and reveal underlying mechanisms [18]. For example, Liu et al. [14]. demonstrated that irrigation volume was the most critical factor influencing agricultural yield (16.71%), followed by planting time (8.53%) and irrigation timing (6.94%). Integrating genetic algorithms to optimize RF hyperparameters further enhances model accuracy, offering a refined approach to evaluating factor importance [19]. This synergy not only improves model performance, but also provides valuable insights into the multifactorial interactions governing complex systems.

Expanding on the understanding of how reclaimed water irrigation influences nitrogen and salt dynamics in agricultural and agroforestry ecosystems, this study aims to (1) develop a machine learning framework integrating genetic algorithms with the random forest model to predict soil nitrogen (NO_3^--N, NH_4^+-N, TN) and salinity (EC, Cl^-) dynamics

with precision; (2) quantify the relative contributions of key factors—such as water quality, irrigation practices, soil properties, and land use patterns—to soil nutrient and salinity accumulation through feature importance analysis; and (3) investigate the regulatory roles of land use and irrigation duration, elucidating their combined effects on soil nitrogen and salinity processes. The findings will provide a robust scientific foundation for optimizing land management practices and reclaimed water irrigation strategies, contributing to the sustainable development of agricultural and agroforestry systems.

2. Materials and Methods

2.1. Sampling Experiments

This study was conducted in a typical water-scarce city in eastern China. This city has many years of experience in using reclaimed water irrigation. The meteorological data of the study area in 2023 are shown in Table 1. In August 2023, 51 soil sampling points were selected through visits and surveys in the study area. Soil samples were collected from woodland, shrubland, grassland, and farmland areas, reflecting the primary land use types under reclaimed water irrigation (Figure 1). The main crops grown on the farmland were soybeans and rice. These sampling points covered different reclaimed water irrigation years including 0, 2, 5, 6, 8, 12, 16, and 18 years. Except for the sample points where reclaimed water irrigation for farmland had only been used for 2 years, the rest of the land was irrigated with reclaimed water covering all irrigation years (0, 2, 5, 6, 8, 12, 16, and 18 years). Soil samples were collected from 0–20, 20–40, and 40–60 cm soil layers, totaling 153 soil samples. The number of soil samples for woodland, shrubland, grassland, and farmland was 36, 36, 63, and 18 respectively. At each sampling point, 1000 g of disturbed soil samples were collected to determine the physical and chemical properties of the soil. Meanwhile, undisturbed soil samples were taken from each layer using a cutting ring, resulting in 153 undisturbed samples.

Table 1. Meteorological data of the study area in 2023.

Month	Average Temperature (°C)	Maximum Temperature (°C)	Minimum Temperature (°C)	Precipitation (mm)	Net Solar Radiation Intensity (Net, MJ/m^2/d)
Jan	2.0	16.12	−9.23	18.88	9.61
Feb	4.1	14.95	−3.54	31.46	10.64
Mar	11.83	25.7	−0.15	24.36	15.33
Apr	15.63	29.66	5.47	77.98	15.69
May	20.96	32.01	9.55	81.12	16.46
Jun	25.73	35.86	15.58	59.08	16.83
Jul	28.02	34.87	22.74	256.52	13.74
Aug	26.85	34.07	19.24	169.95	15.96
Sep	22.98	30.41	14.26	174.36	12.30
Oct	17.88	26.46	7.64	9.35	12.58
Nov	9.72	27.57	−3.62	16.17	9.54
Dec	2.64	20.89	−9.48	29.12	7.76

For reclaimed water, biochemical oxygen demand was determined using the dilution and seeding method. TN was measured using the alkaline potassium persulfate digestion UV spectrophotometric method, and total phosphorus was assessed using the ammonium spectrophotometric method. Suspended solids were quantified using the gravimetric method. Petroleum content was determined through infrared spectrophotometry. Ammonia nitrogen was measured with Nessler's reagent spectrophotometry. Chemical oxygen demand was determined using the dichromate method, while fecal coliform levels were

assessed through manifold zymotechnics. Anionic surfactants were quantified using the methylene blue spectrophotometric method. The water quality data from the reclaimed water plants were collected based on the reclaimed water sources at the sampling points.



Figure 1. Overview of land use types in the experiments: grassland, shrubland, woodland, and farmland.

Soil samples contained in steel cutting rings were used to measure bulk density and saturated hydraulic conductivity using oven-drying and constant-head methods, respectively [20]. Soil particle size was analyzed with a laser particle size analyzer (Bettersize 2000, Dandong Baite Instrument Co., Ltd., Dandong, China), classifyin g particles into clay (0–2 μm), silt (2–20 μm), and sand (20–2000 μm) fractions [21]. Soil organic matter (SOM) was determined using the dichromate oxidation method [22]. Soil pH was measured in a 1:5 soil-to-water suspension with a pH meter (PHS-3E, Shanghai Leici Instrument Co., Ltd., Shanghai, China). Concentrations of NH_4^+-N, NO_3^--N, and TN were analyzed using a Discrete Auto Analyzer (Smartchem200, Alliance, Paris, France) and a Kjeldahl Distillation Unit (K9840, Shanghai Lijing Scientific Instrument Co., Ltd., Shanghai, China) [23,24]. Dissolved organic carbon (DOC), electrical conductivity (EC), and chloride ion (Cl^-) were measured using a Total Organic Carbon Analyzer (TNM-L ROHS, Shimadzu, Kyoto, Japan), an Electrical Conductivity Meter (DDS-307A, INESA, Shanghai Leici Instrument Co., Ltd., Shanghai, China), and an Ion Meter (PXSJ-216F, Shanghai Leici Instrument Co., Ltd., Shanghai, China), respectively [25].

2.2. Research Methods

This study presents the development of two genetic-algorithm-optimized random forest models (GA-RF) to predict dynamic changes in soil nitrogen and salinity levels under reclaimed water irrigation. GA-RF1 predicts soil nitrogen concentrations, including nitrate nitrogen (NO_3^--N), ammonium nitrogen (NH_4^+-N), and total nitrogen (TN), while GA-RF2 focuses on salinity indicators, including electrical conductivity (EC) and chloride ions (Cl^-). Data were acquired through comprehensive soil and water quality monitoring across diverse irrigation durations (irrigation years: 0, 2, 5, 6, 8, 12, 16, and 18 years) and land use types (woodland, shrubland, grassland, and farmland), encompassing a broad suite of physical, chemical, and biological parameters. These include irrigation duration, soil depth, bulk density, organic matter content, soil particle composition (clay, silt, and sand), land use type, and water quality metrics such as biochemical oxygen demand (BOD_5), total nitrogen, total phosphorus, suspended solids, petroleum hydrocarbons, ammonium nitrogen, chemical oxygen demand (COD), fecal coliforms, and anionic surfactants.

To ensure model accuracy, rigorous data preprocessing was undertaken using Pandas and NumPy. Numerical variables, including soil physicochemical properties and water quality parameters, were standardized using the StandardScaler tool from the Scikit-learn library. The standardization method applied was Z-score standardization. Categorical

variables, such as land use types, were encoded as binary features using one-hot encoding, enabling the effective incorporation of discrete characteristics. The dataset was subsequently partitioned into training (80%, 122 samples) and testing (20%, 31 samples) subsets to ensure data randomness and reproducibility.

In GA-RF model construction, model optimization leveraged genetic algorithms (GAs) to refine key parameters of the random forest models, specifically the number of decision trees (n_estimators) and their maximum depth (max_depth). Implemented using the Distributed Evolutionary Algorithms in Python (DEAP) framework, the GA simulated natural selection through iterative selection, crossover, and mutation processes. Parameter ranges were defined as 50–300 for n_estimators and 5–20 for max_depth. The initial population comprised 10 individuals evolving over 10 generations with a crossover probability of 50% and a mutation probability of 20%. Tournament selection, involving competition among three randomly selected individuals, guided evolutionary advancement, with mean squared error (MSE) serving as the fitness criterion. Optimization yielded the best parameter sets: n_estimators = 56 and max_depth = 13 for GA-RF1, and n_estimators = 157 and max_depth = 10 for GA-RF2. These optimized configurations were employed to train the random forest models using the Scikit-learn RandomForestRegressor, with predictions subsequently tested on independent data subsets.

To enhance the reliability of predictions, Bayesian regression was applied as a post-processing step using the Scikit-learn BayesianRidge module. This approach incorporated random forest predictions as inputs, providing both mean predictions and uncertainty estimates in the form of standard deviations. This integrated approach not only refined predictive accuracy, but also facilitated uncertainty quantification, adding an important layer of interpretability. The performance of GA-RF1 and GA-RF2 was assessed through the Nash–Sutcliffe efficiency coefficient (NSE) and Root Mean Square Error (RMSE):

$$NSE = 1 - \frac{\sum_{i=1}^{n} (O_i - S_i)^2}{\sum_{i=1}^{n} \left(O_i - \overline{O}\right)^2} \quad (1)$$

$$RMSE = \sqrt{\frac{\sum_{i=1}^{n} (O_i - S_i)^2}{n}} \quad (2)$$

where O_i is the i observed value; S_i is the i predicted value; $\overline{O}$ and $\overline{S}$ are the mean of all observed and predicted values, respectively; and n is the sample size. When NSE = 1, it indicates a perfect match between observed and predicted values. A value of $0 < NSE < 1$ suggests the model performance is within an acceptable range, whereas $NSE \leq 0$ indicates a poor agreement between predicted and observed values. A smaller RMSE signifies better model performance, reflecting higher simulation accuracy.

To evaluate the influence of key factors on soil nitrogen and salinity accumulation, Shapley Additive Explanation (SHAP) values were applied to quantify their contributions [26,27]. SHAP-based feature importance rankings identified how specific factors, such as irrigation duration and land use types, directly influence nitrogen and salinity accumulation patterns in soils.

Two visualization methods were employed to analyze the spatial and temporal variations in soil properties under reclaimed water irrigation. Contour plots were used to illustrate the distribution and trends of key soil parameters (e.g., NO_3^--N, NH_4^+-N, TN, EC, and Cl^-) across different sampling depths and irrigation durations. Using cubic interpolation, discrete data points were smoothed into a grid, revealing gradients and patterns

through color gradients and contour lines that highlighted the intensity and variation of these parameters. Regression plots were created to explore relationships between soil properties and factors such as irrigation duration and sampling depth. Separate regression analyses for different land use types visually represented trends and variability using scatter plots and regression lines.

The visualizations were implemented using Python 3.11.5 (packaged by Anaconda, Inc.) and built with Matplotlib 3.7.2, SciPy 1.11.1, Seaborn 0.12.2, and SHAP 0.46.0, ensuring clear and interpretable data analysis. For data preprocessing, Pandas 2.2.3 and NumPy 1.25.2 were used, while Scikit-learn 1.5.2 was employed for numerical standardization and model training. Model optimization was conducted with DEAP 1.4, utilizing genetic algorithms to refine random forest hyperparameters.

3. Results

3.1. Model Performance

3.1.1. Training Data Evaluation

The GA-RF model demonstrates strong predictive performance for soil nitrogen (GA-RF 1) and salinity (GA-RF 2) content following irrigation with reclaimed water (Figure 2). Notably, it captures fluctuations within high-peak regions with precision. For nitrogen variables, the training set RMSE decreased from an initial 1.2 to approximately 0.4, while the test set RMSE declined from 1.2 to around 1.0, stabilizing after the addition of 100 trees (Figure 3). This trend suggests that increasing the number of trees effectively reduces error while enhancing generalizability. For salinity variables, the training set RMSE showed a sharp drop from 30 to 5, with test set RMSE decreasing from 30 to 25, eventually reaching stability. The consistent RMSE across both training and test sets indicates robust fitting and generalization, with no overfitting observed.

3.1.2. Test Data Evaluation

Figure 4 compares the predictions of the GA-RF model with the observed values of soil nitrogen (GA-RF 1) and salinity (GA-RF 2) under reclaimed water irrigation using a 95% confidence interval. For GA-RF 1, the Nash coefficients for NO_3^--N, NH_4^+-N, and TN predictions were 0.918, 0.946, and 0.936, respectively, with RMSE values of 1.130 mg/kg, 0.701 mg/kg, and 0.357 g/kg. The highest prediction uncertainties were observed at sample points 17 (grassland, irrigation duration: 16 years), 27 (shrubland, irrigation duration: 12 years), and 28 (grassland, irrigation duration: 16 years), with confidence interval ranges of 1.546–1.649 mg/kg, 0.962–1.039 mg/kg, and 0.491–0.535 g/kg for NO_3^--N, NH_4^+-N, and TN, respectively. For GA-RF 2, the Nash coefficients for EC and Cl^- predictions were 0.967 and 0.887, respectively, with RMSE values of 21,316 μS/cm and 2.077 g/kg. The greatest prediction uncertainties for EC and Cl^- were found at sample points 6 and 20 (farmland, irrigation duration: 2 years), with confidence interval ranges of 28,494–29,065 μS/cm and 3.043–2.962 g/kg, respectively. Overall, the GA-RF 1 and GA-RF 2 models demonstrated strong agreement between predicted and observed values across most samples. These findings underscore the models' effectiveness in processing stable datasets, as indicated by low errors and narrow confidence intervals. However, in regions with extreme values, the prediction performance declined, as evidenced by larger deviations and significantly expanded confidence intervals.

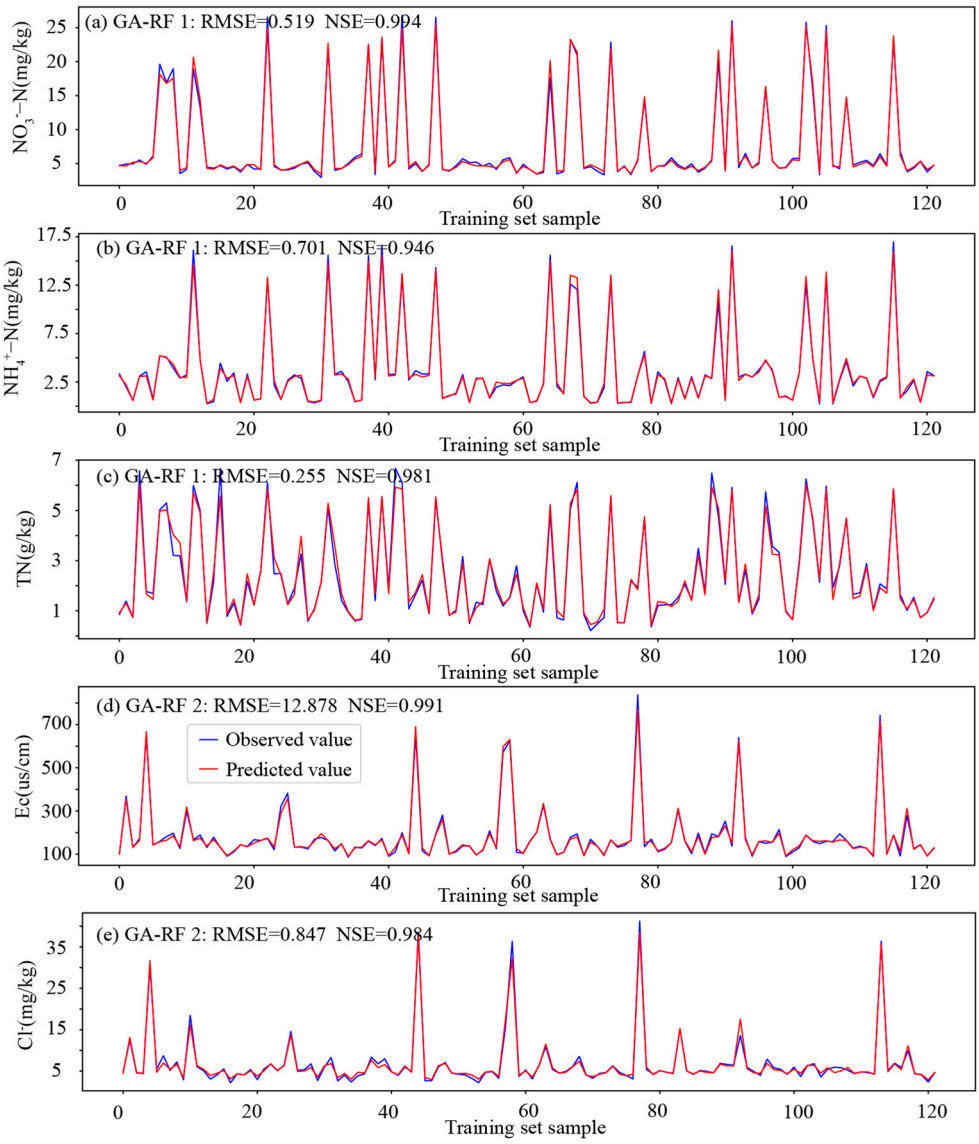


Figure 2. Predicted soil nitrogen content (GA-RF 1: NO_3^--N, NH_4^+-N, TN) and salinity levels (GA-RF 2: EC, Cl^-) for the training set.

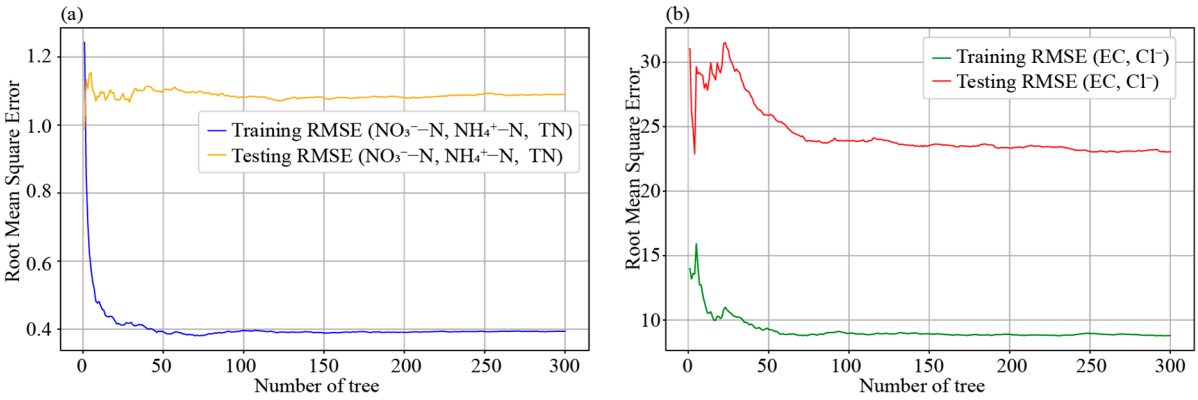


Figure 3. Loss function comparison for training and testing sets: soil nitrogen (GA-RF 1, (**a**)) and salinity (GA-RF 2, (**b**)).

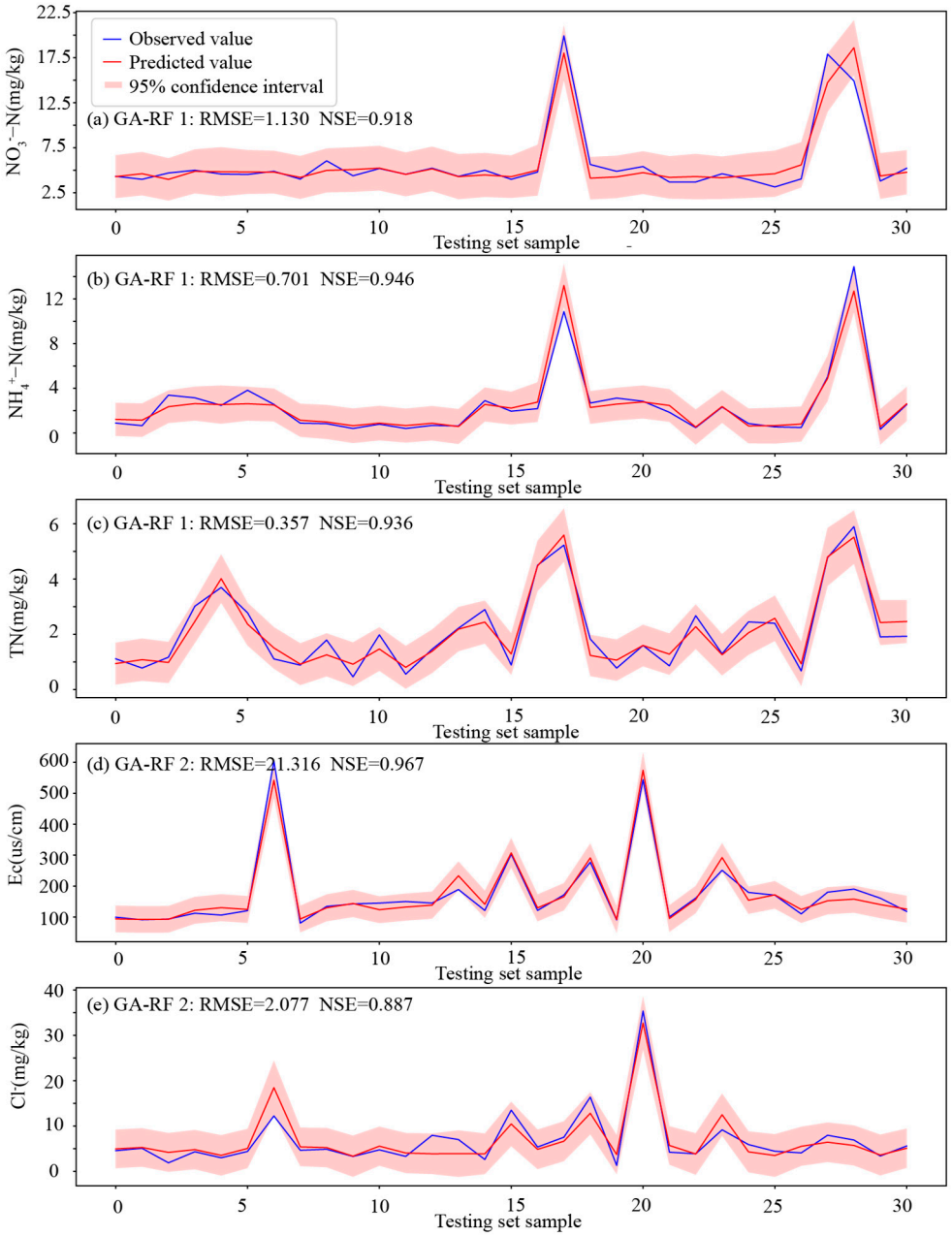


Figure 4. Predicted soil nitrogen content (GA-RF 1: NO_3^--N, NH_4^+-N, TN) and salinity levels (GA-RF 2: EC, Cl^-) for the test set.

3.2. Error Assessment

The error distributions (Figure 5a–e) and residual analyses (Figure 5f–j) for the GA-RF model's predictions of soil nitrogen content (NO_3^--N, NH_4^+-N, TN) and salinity levels (EC, Cl^-) are presented. The error distributions for all variables are centered around zero, reflecting minimal systematic bias in the model's predictions. The relatively narrow spread of errors highlights the model's precision in capturing the variability of soil properties. Residual analysis further reinforces the model's reliability, as the residuals are randomly distributed around the zero line without discernible patterns or trends. These results collectively demonstrate the model's robustness and effectiveness in predicting soil nitrogen content and salinity levels under reclaimed water irrigation conditions.

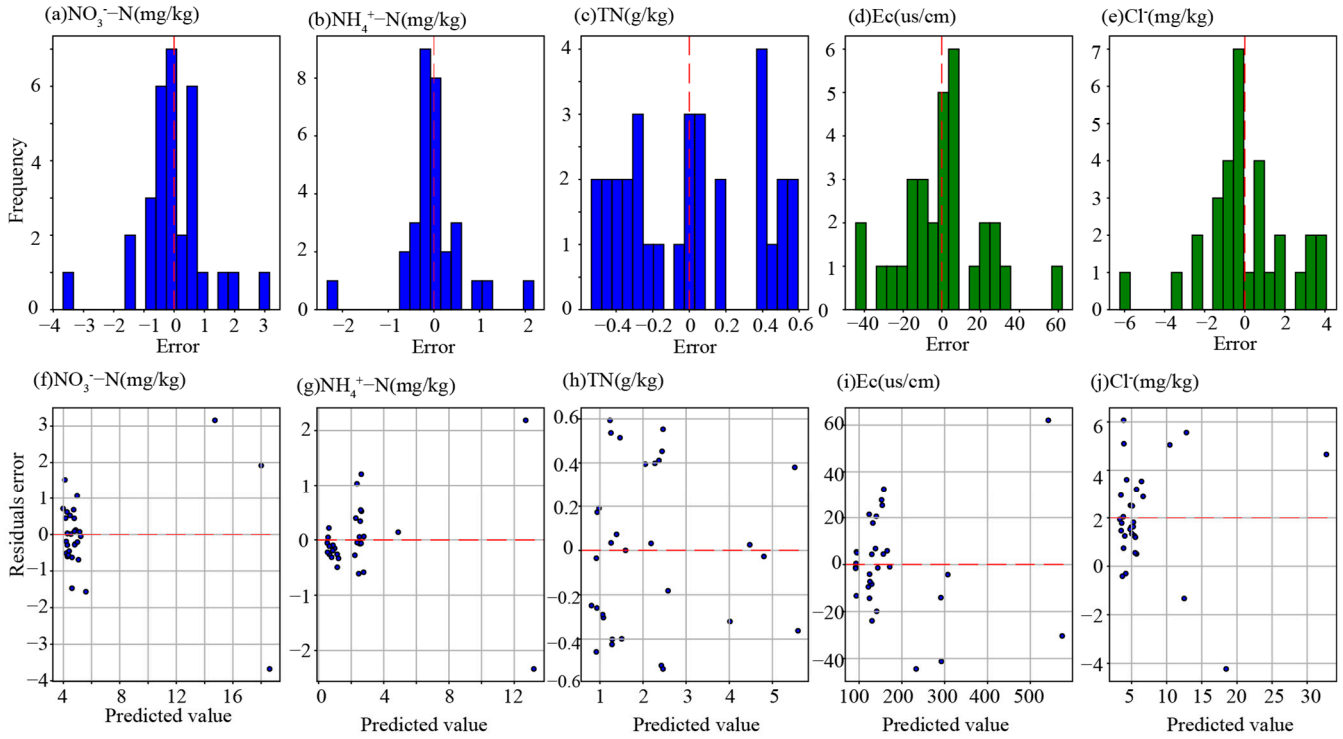


Figure 5. Error distribution (**a**–**e**) and residual analysis(**f**–**j**) for model predictions of soil nitrogen content (GA-RF 1: NO_3^--N, NH_4^+-N, TN) and salinity levels (GA-RF 2: EC, Cl^-).

3.3. Feature Importance Analysis

Figure 6a,b shows that the main factors influencing soil NO_3^--N and NH_4^+-N concentrations after recharge are irrigation duration, fecal coliform levels, and soil depth. The most significant features affecting NO_3^--N and NH_4^+-N are irrigation duration, fecal coliform levels in reclaimed water, and soil depth, respectively. The SHAP values for irrigation duration with respect to NO_3^--N and NH_4^+-N exhibit a "blue-left, red-right" distribution, indicating a positive impact of irrigation duration on these concentrations. In contrast, soil depth has a negative effect, suggesting that NO_3^--N and NH_4^+-N concentrations are highest in shallow soil layers and decrease with increasing depth. Figure 6c indicates that TN is primarily influenced by irrigation duration, fecal coliform levels, and suspended solids concentration in irrigation water. Figure 6d,e reveals that EC and Cl^- concentrations are primarily affected by land use type (especially farmland), as well as chemical oxygen demand, total phosphorus, and total nitrogen in reclaimed water. Farmland has a strong positive effect on EC and Cl^-, likely due to frequent irrigation and fertilization.

3.4. Interaction Effects Analysis

Figure 7 illustrates the distribution patterns of soil nitrogen (NO_3^--N, NH_4^+-N, and TN) and salinity (EC and Cl^-) as influenced by irrigation duration and soil depth following reclaimed water use. NO_3^--N concentrations in the surface soil increase significantly, reaching around 18 mg/kg after over 10 years of irrigation, while deeper layers show a marked decline. Similarly, NH_4^+-N concentrations in shallow soil exhibit a pronounced upward trend with extended irrigation, peaking at approximately 12 mg/kg. TN concentrations reach about 4.8 g/kg in the surface layer and display considerable variability as irrigation duration lengthens. EC shows a complex spatial pattern, with values in shallow areas rising to roughly 180 μS/cm, indicating notable salinity accumulation. Cl^- concentrations also progressively increase in surface soil with prolonged irrigation, peaking at 7.5 mg/kg, reflecting a sustained accumulation trend.

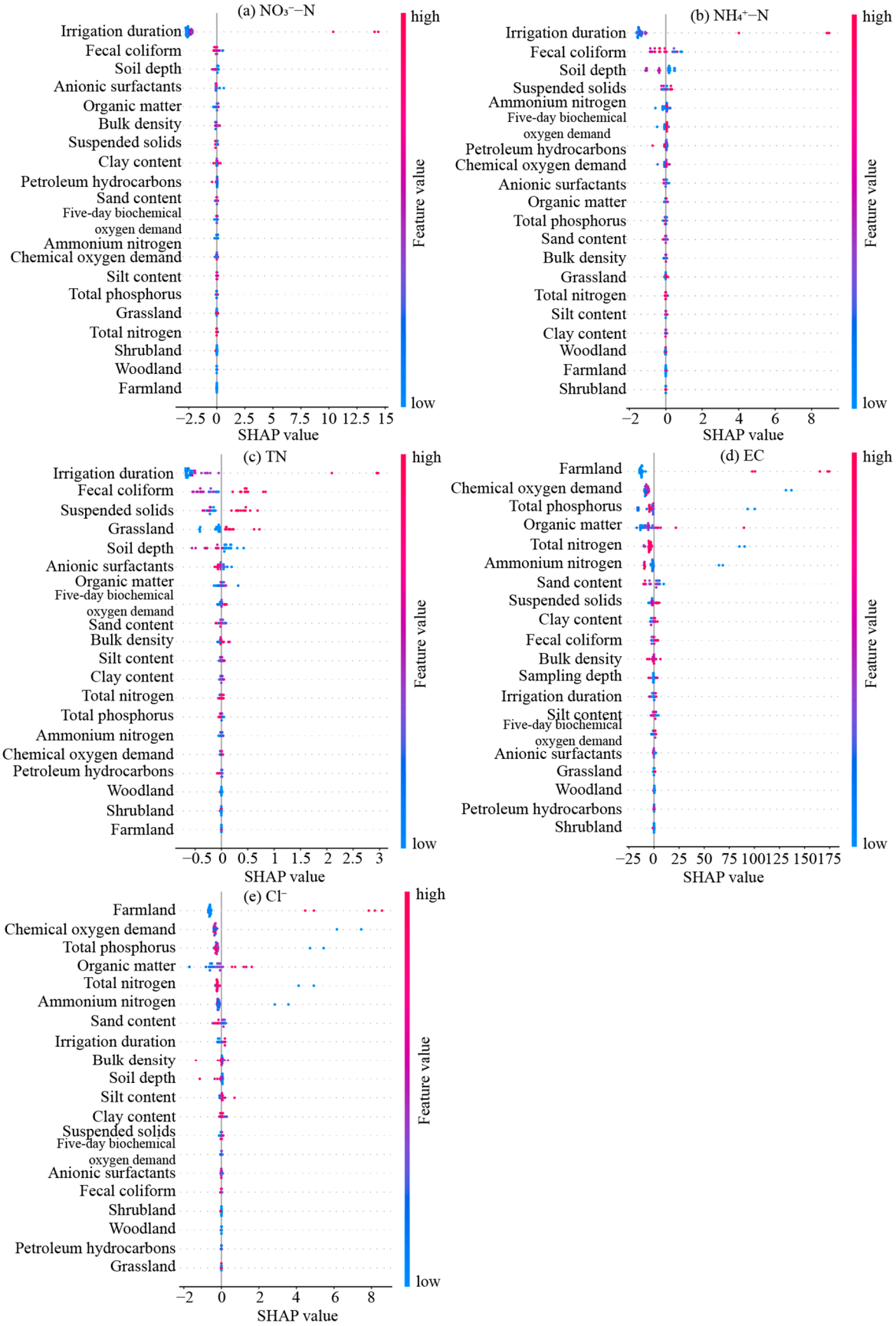


Figure 6. SHAP analysis and feature importance for GA-RF models: GA-RF 1 (**a**–**c**) and GA-RF 2 (**d**,**e**). Color indicates feature values (red: high, blue: low), and the x-axis represents the magnitude and direction of the impact (positive: increase, negative: decrease).

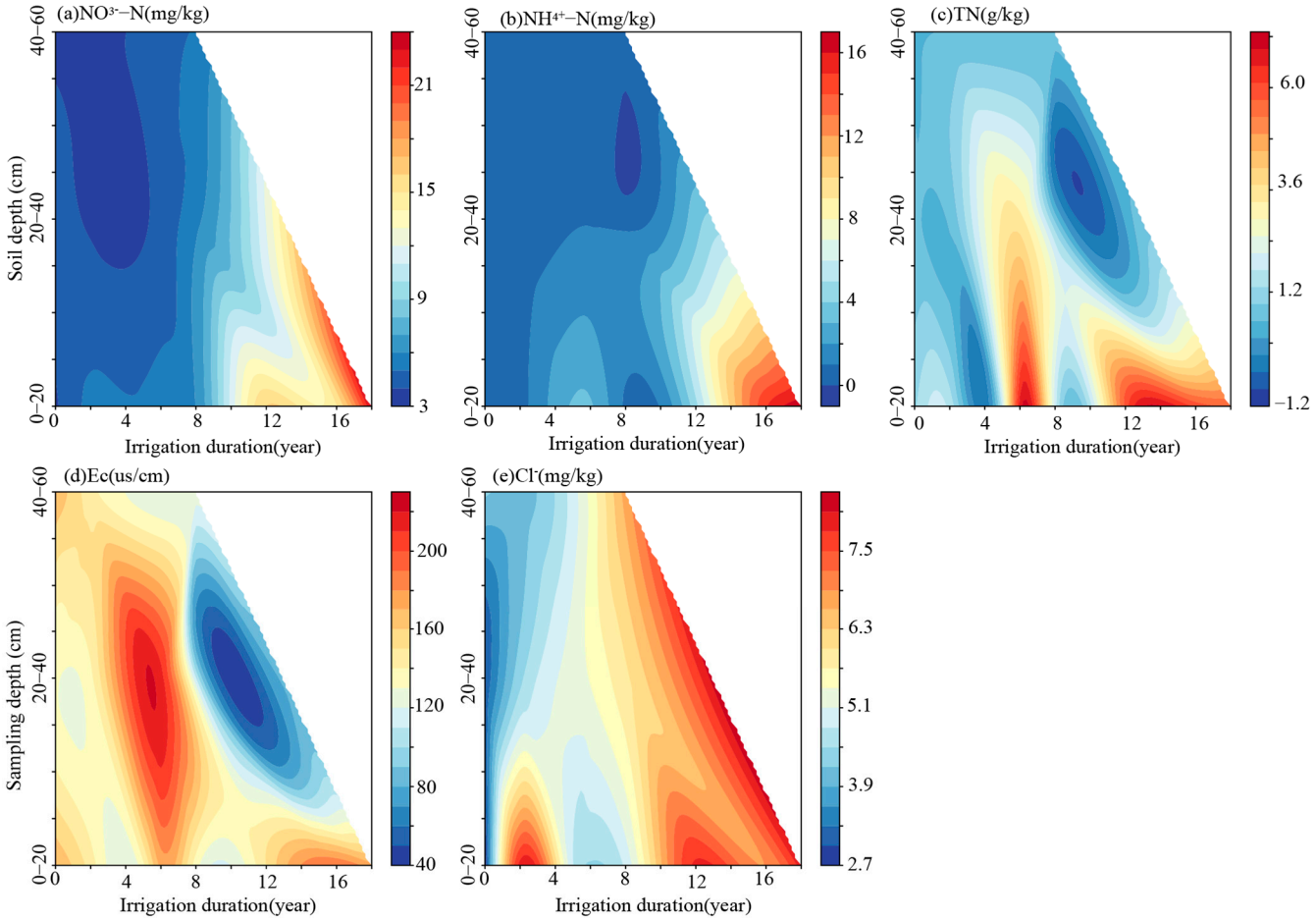


Figure 7. Distribution of NO_3^--N, NH_4^+-N, TN, EC, and Cl^- across different sampling depths and irrigation durations. The color gradient represents the intensity of measured values, with red indicating higher values and blue indicating lower values. Contour lines illustrate the gradient of changes.

Figure 8 depicts the effects of reclaimed water irrigation on soil nitrogen (NO_3^--N, NH_4^+-N, and TN) and salinity (EC and Cl^-) across different soil depths and land use types, including grassland, shrubland, woodland, and farmland. As irrigation duration increases, NO_3^--N and NH_4^+-N concentrations exhibit a steady rise across all land use types, with particularly pronounced accumulation in farmland and woodland, reaching maximum levels of 25 mg/kg and 15 mg/kg, respectively. TN also shows an upward trend, albeit with considerable variability and marked fluctuations. EC in farmland rises sharply during the initial stages, exceeding 700 µS/cm, indicative of significant early salinity accumulation. Cl^- concentration in farmland similarly peaks at over 30 mg/kg. Overall, nitrogen concentrations decline with increasing soil depth, with the steepest decreases observed in both grassland and woodland. In contrast, NO_3^--N and NH_4^+-N levels in farmland remain relatively consistent throughout the soil profile, highlighting substantial accumulation. Furthermore, EC and Cl^- concentrations in farmland are notably higher in the upper soil layers, gradually diminishing with depth, underscoring significant shallow-layer salinity accumulation in farmland soils.

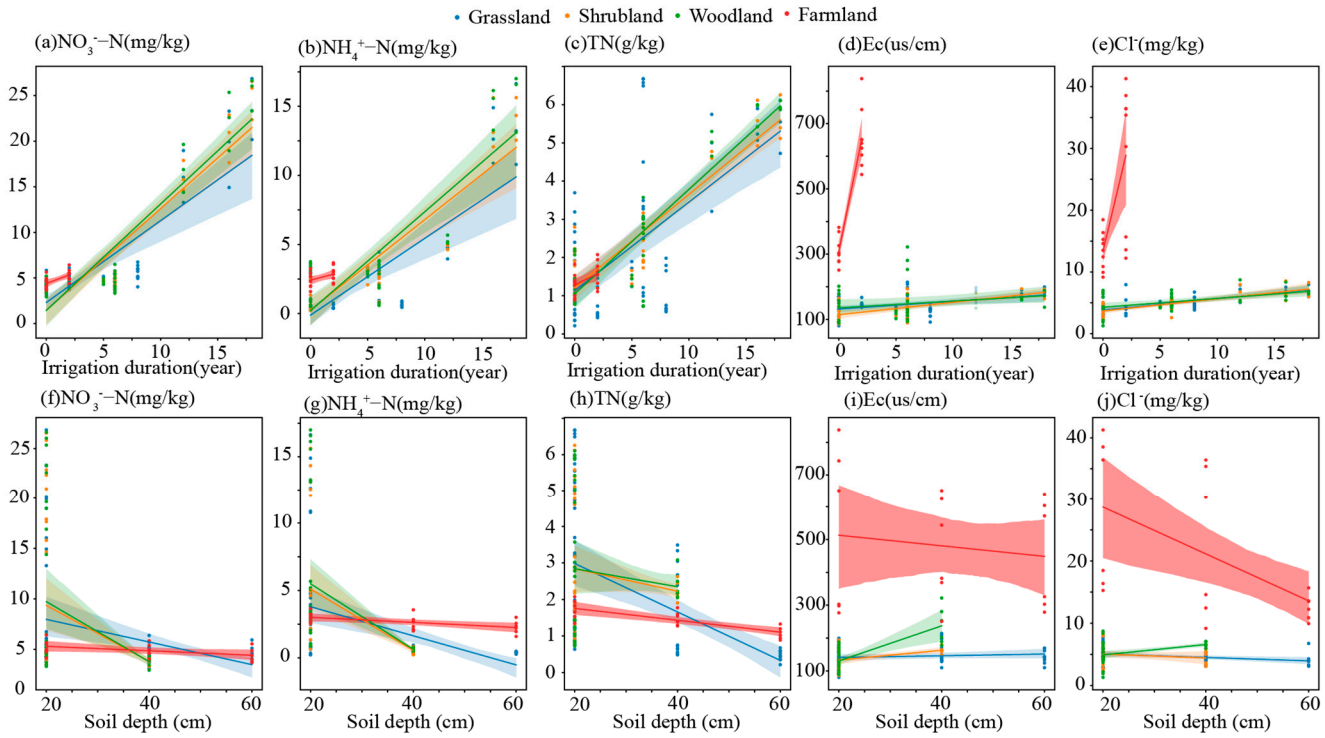


Figure 8. Relationships between NO_3^--N, NH_4^+-N, TN, EC, and Cl^- across different land use types, soil depths, and irrigation durations.

4. Discussion

4.1. Model Accuracy for Soil Nitrogen and Salinity Prediction

The random forest model effectively predicts dynamic changes in soil nitrogen (GA-RF 1) and salinity (GA-RF 2) within the training dataset, demonstrating strong fitting and generalization capabilities, with high adaptability in capturing fundamental fluctuation patterns [28,29]. The model shows low prediction errors for NO_3^--N and NH_4^+-N, while TN exhibits greater variability and reduced accuracy in low-concentration high-variability regions (Figures 3 and 4). This finding aligns with studies by Mola et al. (2024) [30] and Bedbabis et al. (2015) [31], indicating that soil nitrogen dynamics are influenced not only by irrigation duration and sampling depth, but also by soil organic matter and microbial activity. The model's reduced performance with low-concentration TN samples may be due to the complex interactions between inorganic and organic nitrogen forms [32]. In contrast, the RF model performs well for salinity variables (EC and Cl^-) in surface soil, yielding lower overall prediction errors (Figures 3 and 4). However, in high-concentration zones, particularly for EC, error ranges are broader, with some deviations reaching ±100, consistent with [33], who reported challenges in predicting high salinity levels. Reclaimed water irrigation can facilitate salinity migration to deeper soil layers, while high temperatures and arid conditions promote surface salt accumulation via evaporation, exacerbating spatiotemporal variability and complicating model fitting in high-salinity regions [34,35].

Previous research has highlighted the limitations of traditional linear regression models in predicting soil nitrogen and salinity dynamics, particularly when complex nonlinear interactions are involved [36,37]. In contrast, RF models have proven effective in handling multidimensional features and nonlinear relationships, making them well suited for capturing the complexities of soil nutrient and salinity dynamics [18,27]. Nevertheless, Genuer et al. [38] state that RF models can be adversely impacted by redundant or irrelevant features in high-dimensional data, resulting in heightened model complexity, diminished computational efficiency, and potential declines in predictive accuracy, while the selection

of hyperparameters, which traditional methods often fail to optimize, plays a critical role in determining model performance. To address this limitation and enhance model sensitivity, this study focuses on using GA-RF models, which integrate feature selection to improve predictive accuracy and robustness. While advanced deep learning techniques, such as Long Short-Term Memory (LSTM) networks or Convolutional Neural Networks (CNNs), are capable of modeling complex nonlinearities over reclaimed irrigation conditions [39,40], this study specifically opts for RF models due to their computational efficiency and interpretability. RF models offer practical advantages over deep learning methods, especially in terms of data preprocessing and interpretability. They require less preprocessing, making them a more efficient choice given the dataset's size and complexity. When optimized with a genetic algorithm, RF models provide a good balance between complexity and interpretability, helping us understand the interactions between key factors and their impact on nitrogen and salinity dynamics [13,15,41]. While deep learning techniques like LSTM or CNN could improve model performance, we chose RF models for their computational efficiency and ease of use. We also recognize that including spatiotemporal factors, such as weather, soil moisture, and topography, could enhance model accuracy. Future research will explore these variables and consider using advanced neural networks to better understand the long-term effects of reclaimed water irrigation on soil health and crop productivity. Testing these models in different land use and irrigation settings will help strengthen our predictions and support the sustainable use of reclaimed water for irrigation.

4.2. Prediction and Regulation Effect of Soil Nitrogen and Salinity

Under reclaimed water irrigation, soil nitrogen and salinity accumulation are influenced by multiple interrelated factors, including irrigation duration, microbial activity, soil depth, and land use type. This study highlights the complex impacts of reclaimed water components, such as fecal coliforms, chemical oxygen demand, and total phosphorus, on soil nitrogen and salinity dynamics (Figure 6a–c). Microbial populations introduced through reclaimed water, such as fecal coliforms, play a dual role. They can reduce soil NO_3^--N and NH_4^+-N concentrations by promoting denitrification and utilizing ammonium as a nitrogen source [42]. At the same time, these microbes decompose organic matter in the soil, releasing nitrogen and thereby increasing total nitrogen (TN) levels [10,43]. Furthermore, high levels of COD and TP in reclaimed water are metabolized by soil microbes, releasing ions that significantly elevate soil EC and Cl^- concentrations [15].

Irrigation duration and land use are critical factors influencing soil nitrogen and salinity accumulation (Figure 6). Consistent with previous research by Ayoub et al. (2016) [44], our findings demonstrate that prolonged reclaimed water irrigation increases nitrogen and salinity levels in soils. However, the accumulation rates and patterns are strongly dependent on land use types. From the perspective of accumulation rates, forests exhibit the highest levels of NO_3^--N and NH_4^+-N accumulation, driven by the abundance of organic matter and plant residues that enhance nitrogen cycling and retention processes [45]. In contrast, grasslands and shrublands, with their compact soil structures and lower nitrogen demands, display slower nitrogen accumulation rates [46]. Farmland, despite being irrigated for only two years, showed relatively high initial nitrogen levels with a continued upward trend. This rapid accumulation is attributed to the regular application of nitrogen fertilizers, which significantly increase nitrogen inputs. In terms of maximum accumulation, the highest nitrogen and salinity levels were observed across different land use types under reclaimed water irrigation. Grassland soils reached a nitrogen content of 26.85 mg/kg and a TN content of 6.68 g/kg after 18 years of irrigation, while woodland soils recorded a TN content of 17.01 mg/kg over the same period. Importantly, soil TN concentrations

remained within a range sufficient to support healthy crop growth [45], providing essential nutrients without reaching levels that could adversely affect soybean or rice cultivation.

For soil salinity, grasslands, shrublands, and woodlands showed slight increases in salinity levels under 0–18 years of reclaimed water irrigation, while farmland exhibited a significant increase, with soil EC reaching 838 μS/cm and Cl^- content at 41.29 mg/kg after just two years. This disparity highlights the combined influence of land use and irrigation duration on salinity dynamics. The nutrient uptake and salt tolerance of specific crops, such as soybeans and rice, are critical factors that determine their productivity under such irrigation regimes [47–49]. Rice demonstrates high salt tolerance during germination, unaffected at salinity levels as high as 16,300 μS/cm, with severe inhibition observed only above 22,000 μS/cm [50]. However, for the M-202 rice cultivar, salinity as low as 1900 μS/cm can reduce seedling dry weight, and levels of 3400 μS/cm significantly lower seedling survival rates [51]. By comparison, the observed EC of 838 μS/cm in this study is well below these thresholds, indicating minimal impact on rice seed germination and growth. Similarly, soybeans experience delayed germination at low salinity (0.05–0.1% NaCl) and nearly cease growth at 330 mM NaCl, though an 81% germination rate is still observed [52]. The irrigation water in this study, containing 41.29 mg/kg chloride (equivalent to 68.08 mg/L NaCl), has significantly lower salinity, making it unlikely to impair soybean germination or seedling development.

Nonetheless, it is critical to acknowledge the potential for gradual nutrient and salinity accumulation over extended periods (Figures 7 and 8). Prolonged irrigation without proper management could exceed crop tolerance thresholds, particularly in farmland. The continuous monitoring of soil conditions is, therefore, essential to ensure nutrient and salinity levels remain within the acceptable range for soybeans and rice [1,53,54]. Proactive and adaptive management will safeguard long-term crop productivity and promote the sustainable use of reclaimed water in agricultural systems.

4.3. Insights for Optimizing Reclaimed Water Irrigation

To enhance the sustainability and ecological benefits of reclaimed water irrigation across diverse soils and land use types, particularly within agricultural and agroforestry ecosystems, it is essential to optimize management practices that balance irrigation duration, soil properties, and nutrient cycling. By adjusting irrigation duration (season or year) and frequency to suit soil characteristics and crop needs, the risks of excessive nitrogen and salinity accumulation can be mitigated, ensuring that these factors remain within levels conducive to healthy soil and optimal productivity [41]. Tailored irrigation practices not only help maintain soil structure, but also improve nutrient retention and uptake, reducing stress on soils while promoting ecosystem stability [34]. In agroforestry and forested systems, which have a higher buffering capacity due to dense vegetation cover and organic matter cycling, reclaimed water irrigation can be particularly effective in maintaining nutrient balance and promoting soil health. These systems are inherently more resilient to nitrogen and salinity buildup compared to agricultural fields, where more frequent irrigation and fertilization can lead to accumulation. In such fields, integrating reclaimed water irrigation with intermittent freshwater irrigation or alternating sources can help prevent excessive nitrogen loading and salinization [8]. Furthermore, the regular monitoring of soil nitrogen and salinity levels, combined with the adaptive management of irrigation schedules and fertilization, ensures that reclaimed water irrigation remains sustainable and beneficial for crop and tree health [9,44]. In agroforestry systems, where nitrogen tends to accumulate in deeper soil layers, strategies like deep tillage or bioremediation can redistribute nitrogen, reducing the risk of leaching into groundwater while enhancing nutrient availability at root zones. In summary, reclaimed water, when managed with strategically designed

irrigation and nutrient practices tailored to specific land use types and soil properties, provides a sustainable and efficient solution for resource management in agricultural and agroforestry ecosystems.

Despite its advantages, this study was predominantly case-based, focusing on quantifying the impacts of key factors such as water quality, irrigation practices, soil properties, and land use patterns on soil nutrient and salinity dynamics. While these insights are valuable for regions with similar conditions, broader application requires tailored strategies that account for local variations in soil composition, crop tolerance, and water availability. Pilot studies in diverse regions are essential to refine these approaches and validate their effectiveness. Future research should prioritize the development of comprehensive models that integrate soil, vegetation, and water dynamics, enabling better predictions of long-term impacts and optimizing management practices. Precision management, guided by detailed knowledge of soil and land use characteristics, is vital to maximize benefits while mitigating environmental risks. With rigorous scientific validation and site-specific strategies, reclaimed water irrigation holds significant potential as a sustainable solution to water scarcity, fostering resilient agricultural and agroforestry systems globally.

5. Conclusions

Reclaimed water irrigation plays a critical role in addressing global water scarcity, but its long-term impacts on soil nitrogen cycling and salinity dynamics require careful management to prevent adverse effects on agricultural and agroforestry systems. This study highlights the significant accumulation of nitrogen (NO_3^--N, NH_4^+-N, and TN) and salinity (EC and Cl^-) in surface soils with extended irrigation, particularly in farmland, where peak values of NO_3^--N, NH_4^+-N, and EC were observed. In contrast, grassland and woodland soils exhibited minimal accumulation, demonstrating the variability of impacts across land use types. Key factors driving nitrogen accumulation include irrigation duration, fecal coliform levels, and soil depth, while salinity levels were primarily influenced by land use type and the chemical composition of reclaimed water, including COD, total phosphorus, and total nitrogen. These findings emphasize the need for targeted management strategies tailored to specific land use types to mitigate nitrogen and salinity buildup. Future research should prioritize the development of integrated models that incorporate soil, vegetation, and water dynamics to better predict long-term impacts and optimize management practices. Such models will enable a holistic understanding of the interactions within agricultural and agroforestry systems under reclaimed water irrigation, contributing to sustainable resource use and soil health preservation.

Author Contributions: Z.L.: Conceptualization, Methodology, Writing—original draft, Writing—review and editing; K.F.: Investigation, Software; X.S.: Validation, Methodology, Writing—review and editing; Y.W.: Investigation, Software; Z.T.: Validation, Software; J.L.: Investigation, Software; L.B.: Investigation, Software; Q.H.: Conceptualization, Methodology, Writing—original draft, Writing—review and editing. All authors have read and agreed to the published version of the manuscript.

Funding: Research Projects on Natural Resources in Jiangsu Province (2024003) and Innovation and Entrepreneurship Training Program for College Students in Nanjing University of Information Science and Technology (202410300168Y).

Data Availability Statement: The data that support the findings of this study are available from the corresponding author upon reasonable request.

Conflicts of Interest: There is no conflict of interest.

References

1. Berhe, G.T.; Baartman, J.E.M.; Veldwisch, G.J.; Grum, B.; Ritsema, C.J. Irrigation Development and Management Practices in Ethiopia: A Systematic Review on Existing Problems, Sustainability Issues and Future Directions. *Agric. Water Manag.* **2022**, *274*, 107959. [CrossRef]
2. Ward, F.A. Enhancing Climate Resilience of Irrigated Agriculture: A Review. *J. Environ. Manag.* **2022**, *302*, 114032. [CrossRef] [PubMed]
3. Boretti, A.; Rosa, L. Reassessing the Projections of the World Water Development Report. *NPJ Clean Water* **2019**, *2*, 15. [CrossRef]
4. Scanlon, B.R.; Fakhreddine, S.; Rateb, A.; de Graaf, I.; Famiglietti, J.; Gleeson, T.; Grafton, R.Q.; Jobbagy, E.; Kebede, S.; Kolusu, S.R.; et al. Global Water Resources and the Role of Groundwater in a Resilient Water Future. *Nat. Rev. Earth Environ.* **2023**, *4*, 87–101. [CrossRef]
5. Graham, N.T.; Iyer, G.; Wild, T.B.; Dolan, F.; Lamontagne, J.; Calvin, K. Agricultural Market Integration Preserves Future Global Water Resources. *One Earth* **2023**, *6*, 1235–1245. [CrossRef]
6. Seijger, C.; Urfels, A.; Christoforidou, M.; Hellegers, P.; Borghuis, G.; Langan, S.; van Halsema, G. More Food, but Less Land and Water for Nature: Why Agricultural Productivity Gains Did Not Materialize. *Agric. Water Manag.* **2025**, *307*, 109229. [CrossRef]
7. Rosa, L.; Chiarelli, D.D.; Rulli, M.C.; Dell'Angelo, J.; D'Odorico, P. Global Agricultural Economic Water Scarcity. *Sci. Adv.* **2020**, *6*, eaaz6031. [CrossRef]
8. Yerli, C.; Sahin, U.; Ors, S.; Kiziloglu, F.M. Improvement of Water and Crop Productivity of Silage Maize by Irrigation with Different Levels of Recycled Wastewater under Conventional and Zero Tillage Conditions. *Agric. Water Manag.* **2023**, *277*, 108100. [CrossRef]
9. Azad, A.; Liu, H. Pharmaceutical and Personal Care Products in Recycled Water for Edible Crop Irrigation: Understanding the Occurrence, Crop Uptake, and Water Quantity Effects. *Agric. Water Manag.* **2024**, *304*, 109047. [CrossRef]
10. Verma, K.; Manisha, M.; Shivali, N.U.; Santrupt, R.M.; Anirudha, T.P.; Ramesh, N.; Chanakya, H.N.; Parama, V.R.R.; Kumar, M.S.M.; Rao, L. Investigating the Effects of Irrigation with Indirectly Recharged Groundwater Using Recycled Water on Soil and Crops in Semi-Arid Areas. *Environ. Pollut.* **2023**, *337*, 122516. [CrossRef]
11. Liu, M.; Qiao, P.; Shan, Y.; Zhang, Z.; Pan, P.; Li, Y. Migration and Accumulation Simulation Prediction of PPCPs in Urban Green Space Soil Irrigated with Recycled Water: A Review. *J. Hazard. Mater.* **2024**, *476*, 135037. [CrossRef] [PubMed]
12. Dikinya, O.; Areola, O. Comparative Analysis of Heavy Metal Concentration in Secondary Treated Wastewater Irrigated Soils Cultivated by Different Crops. *Int. J. Environ. Sci. Technol.* **2010**, *7*, 337–346. [CrossRef]
13. Rahman, M.M.; Hagare, D.; Maheshwari, B. Framework to Assess Sources Controlling Soil Salinity Resulting from Irrigation Using Recycled Water: An Application of Bayesian Belief Network. *J. Clean. Prod.* **2015**, *105*, 406–419. [CrossRef]
14. Liu, X.; Zhang, L.; Yang, F.; Zhou, W. Determining Reclaimed Water Quality Thresholds and Farming Practices to Improve Food Crop Yield: A Meta-Analysis Combined with Random Forest Model. *Sci. Total Environ.* **2023**, *862*, 160774. [CrossRef]
15. Phogat, V.; Mallants, D.; Cox, J.W.; Simunek, J.; Oliver, D.P.; Pitt, T.; Petrie, P.R. Impact of Long-Term Recycled Water Irrigation on Crop Yield and Soil Chemical Properties. *Agric. Water Manag.* **2020**, *237*, 106167. [CrossRef]
16. Han, Y.; Qiao, D.; Qi, X.; Li, P.; Guo, W. Effects of reclaimed water irrigation levels on soil salinity and composition of soil bacteria community. *Trans. Chin. Soc. Agric. Eng.* **2020**, *36*, 106–117. [CrossRef]
17. Singh, A.; Verdi, A.; Haver, D.; Sapkota, A.; Iradukunda, J.C. Using a Soil Moisture Sensor-Based Smart Controller for Autonomous Irrigation Management of Hybrid Bermudagrass with Recycled Water in Coastal Southern California. *Agric. Water Manag.* **2024**, *299*, 108906. [CrossRef]
18. Park, S.; Im, J.; Jang, E.; Rhee, J. Drought Assessment and Monitoring through Blending of Multi-Sensor Indices Using Machine Learning Approaches for Different Climate Regions. *Agric. For. Meteorol.* **2016**, *216*, 157–169. [CrossRef]
19. Tian, B.; Xiong, W. A Feature Selection Algorithm for Big Data Based on Genetic Algorithm. In *Recent Developments in Mechatronics and Intelligent Robotics*; Qiao, F., Patnaik, S., Wang, J., Eds.; Advances in Intelligent Systems and Computing; Springer International Publishing: Cham, Switzerland, 2018; Volume 690, pp. 159–163, ISBN 978-3-319-65977-0.
20. Ju, X.; Gao, L.; She, D.; Jia, Y.; Pang, Z.; Wang, Y. Impacts of the Soil Pore Structure on Infiltration Characteristics at the Profile Scale in the Red Soil Region. *Soil Tillage Res.* **2024**, *236*, 105922. [CrossRef]
21. Jonasz, M. Size, Shape, Composition, and Structure of Microparticles from Light Scattering. In *Principles, Methods and Application of Particle Size Analysis*; Syvitski, J.P.M., Ed.; Cambridge University Press: Cambridge, UK, 1991; pp. 143–162, ISBN 978-0-521-04461-5.
22. Cai, X.; Wang, T.; Fu, X.; Yan, X.; Zhang, J.; Wang, K.; Liu, Z.; Wen, T.; Sun, W. Comparative study on the determination of organic matter content in soil using potassium dichromate volumetric method and high-frequency infrared carbon sulfur analyzer method. *Soil. Fert. Sci. China* **2024**, *7*, 253–258. [CrossRef]
23. Li, M. Determination of Hydrolyzable Nitrogen—Alkaline Hydrolysis Distillation Method Using Automatic Kjeldahl Nitrogen Analyzer. *Zhejiang Land Resour.* **2023**, *S1*, 107–111. [CrossRef]
24. Lang, Y. Advantages and Limitation of Total Nitrogen Automatic Analyzer in Surface Water Monitoring. *Environ. Sci. Manag.* **2015**, *40*, 158–159+183.

25. Jiang, Y.; Cao, W. Discussion on the Application andmaintenance of Total Organic Carbon Analyzer. *Petrochem. Ind. Technol.* **2024**, *31*, 155–157+163.
26. Lundberg, S.M.; Lee, S.-I. A Unified Approach to Interpreting Model Predictions. In *Advances in Neural Information Processing Systems 30 (NIPS 2017)*; Guyon, I., Luxburg, U.V., Bengio, S., Wallach, H., Fergus, R., Vishwanathan, S., Garnett, R., Eds.; Neural Information Processing Systems (NIPS): La Jolla, CA, USA, 2017; Volume 30.
27. Wang, C.; Liu, J.; Qiu, C.; Su, X.; Ma, N.; Li, J.; Wang, S.; Qu, S. Identifying the Drivers of Chlorophyll-a Dynamics in a Landscape Lake Recharged by Reclaimed Water Using Interpretable Machine Learning. *Sci. Total Environ.* **2024**, *906*, 167483. [CrossRef] [PubMed]
28. Chen, K.; Chen, H.; Zhou, C.; Huang, Y.; Qi, X.; Shen, R.; Liu, F.; Zuo, M.; Zou, X.; Wang, J.; et al. Comparative Analysis of Surface Water Quality Prediction Performance and Identification of Key Water Parameters Using Different Machine Learning Models Based on Big Data. *Water Res.* **2020**, *171*, 115454. [CrossRef]
29. van der Westhuizen, S.; Heuvelink, G.B.M.; Hofmeyr, D.P. Multivariate Random Forest for Digital Soil Mapping. *Geoderma* **2023**, *431*, 116365. [CrossRef]
30. Mola, M.; Kougias, P.G.; Statiris, E.; Papadopoulou, P.; Malamis, S.; Monokrousos, N. Short-Term Effect of Reclaimed Water Irrigation on Soil Health, Plant Growth and the Composition of Soil Microbial Communities. *Sci. Total Environ.* **2024**, *949*, 175107. [CrossRef] [PubMed]
31. Bedbabis, S.; Trigui, D.; Ben Ahmed, C.; Clodoveo, M.L.; Camposeo, S.; Vivaldi, G.A.; Ben Rouina, B. Long-Terms Effects of Irrigation with Treated Municipal Wastewater on Soil, Yield and Olive Oil Quality. *Agric. Water Manag.* **2015**, *160*, 14–21. [CrossRef]
32. Zhu, Y.; Wei, C.; Chi, Y.; Yang, P. The Influencing Mechanisms of Reclaimed Water on N_2O Production in a Multiyear Maize-Wheat Rotation. *Agronomy* **2023**, *13*, 2393. [CrossRef]
33. Lyu, S.; Chen, W.; Wen, X.; Chang, A.C. Integration of HYDRUS-1D and MODFLOW for Evaluating the Dynamics of Salts and Nitrogen in Groundwater under Long-Term Reclaimed Water Irrigation. *Irrig. Sci.* **2019**, *37*, 35–47. [CrossRef]
34. Chen, W.; Lu, S.; Pan, N.; Jiao, W. Impacts of Long-Term Reclaimed Water Irrigation on Soil Salinity Accumulation in Urban Green Land in Beijing. *Water Resour. Res.* **2013**, *49*, 7401–7410. [CrossRef]
35. Mohanavelu, A.; Naganna, S.R.; Al-Ansari, N. Irrigation Induced Salinity and Sodicity Hazards on Soil and Groundwater: An Overview of Its Causes, Impacts and Mitigation Strategies. *Agriculture* **2021**, *11*, 983. [CrossRef]
36. Du, S.; Pan, Q.; Xu, Y.; Cao, S. Comparison of Three Measurement Models of Soil Nitrate-Nitrogen Based on Ion-Selective Electrodes. *Int. J. Agric. Biol. Eng.* **2020**, *13*, 211–216. [CrossRef]
37. Dong, H.; Tian, F. Soil Salinity Inversion Based on a Stacking Integrated Learning Algorithm. *Agriculture* **2024**, *14*, 1777. [CrossRef]
38. Genuer, R.; Poggi, J.-M.; Tuleau-Malot, C. Variable selection using random forests. *Pattern Recognition Letters* **2010**, *31*, 2225–2236. [CrossRef]
39. Gupta, R.; Pothapragada, S.K.; Xu, W.; Goel, P.K.; Barrera, M.A.; Saldanha, M.S.; Harley, J.B.; Morgan, K.T.; Zare, A.; Zotarelli, L. Estimating Soil Mineral Nitrogen from Data-Sparse Field Experiments Using Crop Model-Guided Deep Learning Approach. *Comput. Electron. Agric.* **2024**, *225*, 109355. [CrossRef]
40. Zhong, L.; Guo, X.; Ding, M.; Ye, Y.; Jiang, Y.; Zhu, Q.; Li, J. SHAP Values Accurately Explain the Difference in Modeling Accuracy of Convolution Neural Network between Soil Full-Spectrum and Feature-Spectrum. *Comput. Electron. Agric.* **2024**, *217*, 108627. [CrossRef]
41. Nicolas, E.; Alarcon, J.J.; Mounzer, O.; Pedrero, F.; Nortes, P.A.; Alcobendas, R.; Romero-Trigueros, C.; Bayona, J.M.; Maestre-Valero, J.F. Long-Term Physiological and Agronomic Responses of Mandarin Trees to Irrigation with Saline Reclaimed Water. *Agric. Water Manag.* **2016**, *166*, 1–8. [CrossRef]
42. Ofori, S.; Puskacova, A.; Ruzickova, I.; Wanner, J. Treated Wastewater Reuse for Irrigation: Pros and Cons. *Sci. Total Environ.* **2021**, *760*, 144026. [CrossRef]
43. Wu, W.; Ma, M.; Hu, Y.; Yu, W.; Liu, H.; Bao, Z. The Fate and Impacts of Pharmaceuticals and Personal Care Products and Microbes in Agricultural Soils with Long Term Irrigation with Reclaimed Water. *Agric. Water Manag.* **2021**, *251*, 106862. [CrossRef]
44. Ayoub, S.; Al-Shdiefat, S.; Rawashdeh, H.; Bashabsheh, I. Utilization of Reclaimed Wastewater for Olive Irrigation: Effect on Soil Properties, Tree Growth, Yield and Oil Content. *Agric. Water Manag.* **2016**, *176*, 163–169. [CrossRef]
45. Tung, G.P.; Hung, T.N.; Kappas, M. Assessment of Soil Quality Indicators under Different Agricultural Land Uses and Topographic Aspects in Central Vietnam. *Int. Soil Water Conserv. Res.* **2018**, *6*, 280–288. [CrossRef]
46. Liu, D.; Huang, Y.; An, S.; Sun, H.; Bhople, P.; Chen, Z. Soil Physicochemical and Microbial Characteristics of Contrasting Land-Use Types along Soil Depth Gradients. *Catena* **2018**, *162*, 345–353. [CrossRef]
47. Liu, T.Q.; Fan, D.J.; Zhang, X.X.; Chen, J.; Li, C.F.; Cao, C.G. Deep Placement of Nitrogen Fertilizers Reduces Ammonia Volatilization and Increases Nitrogen Utilization Efficiency in No-Tillage Paddy Fields in Central China. *Field Crop. Res.* **2015**, *184*, 80–90. [CrossRef]

48. Reddy, I.N.B.L.; Kim, B.-K.; Yoon, I.-S.; Kim, K.-H.; Kwon, T.-R. Salt Tolerance in Rice: Focus on Mechanisms and Approaches. *Rice Sci.* **2017**, *24*, 123–144. [CrossRef]
49. Lindberg, S.; Premkumar, A. Ion Changes and Signaling under Salt Stress in Wheat and Other Important Crops. *Plants* **2024**, *13*, 46. [CrossRef] [PubMed]
50. Heenan, D.P.; Lewin, L.G.; McCaffery, D.W. Salinity Tolerance in Rice Varieties at Different Growth Stages. *Aust. J. Exp. Agric.* **1988**, *28*, 343–349. [CrossRef]
51. Zeng, L.H.; Shannon, M.C. Salinity Effects on Seedling Growth and Yield Components of Rice. *Crop Sci.* **2000**, *40*, 996–1003. [CrossRef]
52. Zhang, W.; Liao, X.; Yu, D.; Kan, G. A review of salt tolerance in soybean (*Glycine max* (L.) Merill). *Soils Crops* **2018**, *7*, 284–292. [CrossRef]
53. Cakmakci, T.; Sahin, U. Productivity and Heavy Metal Pollution Management in a Silage Maize Field with Reduced Recycled Wastewater Applications with Different Irrigation Methods. *J. Environ. Manag.* **2021**, *291*, 112602. [CrossRef] [PubMed]
54. He, Z.; Hu, Q.; Zhang, Y.; Cao, H.; Nan, X. Effects of Irrigation and Nitrogen Management Strategies on Soil Nitrogen and Apple Yields in Loess Plateau of China. *Agric. Water Manag.* **2023**, *280*, 108220. [CrossRef]

Disclaimer/Publisher's Note: The statements, opinions and data contained in all publications are solely those of the individual author(s) and contributor(s) and not of MDPI and/or the editor(s). MDPI and/or the editor(s) disclaim responsibility for any injury to people or property resulting from any ideas, methods, instructions or products referred to in the content.